Modeling of the Carbon Dioxide Solubility in Imidazolium-Based Ionic Liquids with the tPC-PSAFT Equation of State

Maaike C. Kroon,*,†,‡ Eirini K. Karakatsani,§ Ioannis G. Economou,*,§ Geert-Jan Witkamp,‡ and Cor J. Peters*,†

Physical Chemistry and Molecular Thermodynamics, Department of Chemical Technology, Faculty of Applied Sciences, Delft University of Technology, Julianalaan 136, 2628 BL Delft, The Netherlands, Laboratory for Process Equipment, Department of Process & Energy, Faculty of Mechanical, Maritime, and Materials Engineering, Delft University of Technology, Leeghwaterstraat 44, 2628 CA Delft, The Netherlands, and Molecular Thermodynamics and Modeling of Materials Laboratory, Institute of Physical Chemistry, National Center for Scientific Research "Demokritos", GR-15310 Aghia Paraskevi Attikis, Greece

In this work, an equation of state (EoS) is developed to predict accurately the phase behavior of ionic liquid + CO_2 systems based on the truncated perturbed chain polar statistical associating fluid theory (tPC-PSAFT) EoS. This EoS accounts explicitly for the dipolar interactions between ionic liquid molecules, the quadrupolar interactions between CO_2 molecules, and the Lewis acid–base type of association between the ionic liquid and the CO_2 molecules. Physically meaningful model pure-component parameters for ionic liquids are estimated based on literature data. All experimental vapor–liquid equilibrium data are correlated with a single linearly temperature-dependent binary interaction parameter. The ability of the model to describe accurately carbon dioxide solubility in various 1-alkyl-3-methylimidazolium-based ionic liquids with different alkyl chain lengths and different anions at pressures from 0 to 100 MPa and carbon dioxide fractions from 0 to 75 mol % is demonstrated. In all cases, good agreement with experimental data is obtained.

Introduction

In the past decade, ionic liquids (ILs) have received much attention for use as environmentally benign reaction and separation media.[1–4] ILs are molten salts with melting points close to room temperature. Their most remarkable property is that their vapor pressure is negligibly small, which means that ILs are nonvolatile, nonflammable, and odorless. Other characteristics of ILs include a wide liquid temperature range, a high thermal and electrochemical stability, a high ionic conductivity, and good solvency properties. In principle, ILs can be tailored for a specific application by the right choice of cation and anion.

ILs are increasingly used as novel processing media in combination with supercritical carbon dioxide (CO_2). Because of the negligible vapor pressure, it is possible to extract organic products from ILs by using supercritical carbon dioxide without any contamination by the IL.[5–7] Subsequently, this separation step is combined with homogeneously catalyzed reactions in IL/CO_2 biphasic solutions, where the catalyzed reaction takes place in the IL phase and the product is separated by extraction into the CO_2 phase.[8–13] Further process development requires data on vapor–liquid equilibria of mixtures of ILs and CO_2.

In the past few years, a growing number of measurements reporting CO_2 solubility in various ILs have become available.[7,14–24] Research in our Delft groups has shown that CO_2 is highly soluble in different alkylmethylimidazolium-based ILs

combined with tetrafluoroborate and hexafluorophosphate anions at lower pressures, and that bubble-point pressures sharply increase at higher mole fractions of CO_2.[19–23] It was also shown that a larger alkyl group of the alkylmethylimidazolium cation leads to higher solubilities of CO_2 in the ionic liquid.[24]

Although experimental data on CO_2 solubility in ILs are available in the literature, more data are needed for process design, and their experimental determination is often difficult, time-consuming, and expensive. Therefore, it is highly desirable to develop predictive methods for estimating the CO_2 solubility in ILs over a wide range of conditions. Different approaches were proposed for modeling the phase behavior of IL + CO_2 systems. At the molecular level, CO_2 solubilities in ILs were predicted using Monte Carlo simulation techniques.[25–27] Molecular simulation allows elucidation of microscopic phenomena that control macroscopic physical properties. In this respect, molecular dynamics simulation was used to investigate the solvation dynamics of CO_2 in ILs, and it was shown that CO_2 occupies the cavities in the IL phase.[28,29] At a more coarse-grained level, Lee[30] and Carda-Broch et al.[31] used a linear solvation energy relationship in solute parameters in order to analyze the CO_2 solvation in ILs. The irregular ionic lattice model was applied to predict CO_2 solubility in ILs by Ally et al.[32] Furthermore, Scovazzo et al.[33] used regular solution theory for this purpose.

Equations of state (EoS) have also been used for modeling the ILs phase behavior in CO_2 and other solvents. All of these efforts have been restricted to low and medium pressure, and applications to IL + CO_2 mixtures close to or above 100 MPa are nonexistent. Shiflett et al.[34] used the Redlich–Kwong EoS for modeling of the CO_2 solubility in 1-butyl-3-methylimidazolium tetrafluoroborate [bmim⁺][BF₄⁻] and 1-butyl-3-meth-

* Corresponding authors. E-mail: Economou@chem.demokritos.gr (I.G.E.); C.J.Peters@tnw.tudelft.nl (C.J.P); m.c.kroon@tnw.tudelft.nl (M.C.K.).
† Department of Chemical Technology, Faculty of Applied Sciences, Delft University of Technology.
‡ Department of Process & Energy, Faculty of Mechanical, Maritime and Materials Engineering, Delft University of Technology.
§ National Center for Scientific Research "Demokritos".

CO2 Solubility in Imidazolium-Based Ionic Liquids

J. Phys. Chem. B, Vol. 110, No. 18, 2006 **9263**

ylimidazolium hexafluorophosphate [bmim$^+$][PF$_6^-$] at pressures under 2 MPa (vapor−liquid equilibrium; VLE). However, at higher pressures, this EoS cannot accurately predict the phase behavior of IL + CO$_2$ systems. Shariati et al.[35] used the Peng−Robinson EoS in order to model the phase behavior of the 1-ethyl-3-methylimidazolium hexafluorophosphate [emim$^+$][PF$_6^-$] + fluoroform binary system (VLE), but also this EoS was not able to accurately describe the completely different phase behavior of [emim$^+$][PF$_6^-$] + CO$_2$.[19] Furthermore, binary IL + water systems (liquid−liquid equilibrium; LLE) have been modeled by using the NRTL EoS[36] and excess Gibbs energy methods.[37] Ternary IL + alcohol + alkane systems have been modeled using the UNIQUAC EoS.[38]

In this work, an EoS is developed in order to accurately predict the phase behavior of imidazolium-based ILs + CO$_2$ systems up to high pressures (100 MPa). To obtain a model capable to capture accurately both the low- and the high-pressure phase behavior, a statistical mechanics-based EoS is used that accounts explicitly for the microscopic characteristics of ILs and CO$_2$. The cation and the anion of the IL form an ion pair in the melt due to Coulomb interactions that keep them closely associated, even in systems diluted with CO$_2$.[39−41] Therefore, IL molecules are considered to be highly asymmetric neutral ion pairs with a large dipole moment as a result of the charge distribution over the ion pair.[1,42] Moreover, CO$_2$ molecules have a quadrupole moment.[43] The EoS proposed here should, therefore, take the polar interactions between the IL molecules and the CO$_2$ molecules explicitly into account. Also, evidence of a strong association between the CO$_2$ and the anion of the IL was found.[44] Kazarian et al.[45] found that this association is probably the result of a Lewis acid−base interaction between the CO$_2$ and the anions of the ILs, where the CO$_2$ acts as a Lewis acid and the anions act as Lewis bases. Huang et al.[29] claim that this association is due to the strong charge-quadrupole moment interaction between CO$_2$ and the anions. In all cases, this association should also be accounted for in the EoS.

A model suitable for the purposes outlined above is rooted to the statistical associating fluid theory (SAFT),[46−49] which is based on Wertheim's first-order thermodynamic perturbation theory (TPT1).[50−53] The original SAFT EoS uses a chain of hard spheres, with short-range directional forces accounting for hydrogen bonding (association) as reference fluid, and treats the dispersive interactions as a perturbation to the reference fluid. However, the SAFT EoS accounts for the chainlike shape of the molecules only in the repulsive contribution. In one of the most successful modifications, the perturbed chain-SAFT (PC-SAFT), the chain-length dependence of the dispersive interactions, is also accounted for, resulting in a more accurate model for chain molecules.[54]

Several groups have extended the SAFT EoS and the PC-SAFT EoS in order to incorporate multipolar interactions, where the long-ranged multipolar forces (together with the dispersive forces) were considered as a perturbation over the short-range forces that almost exclusively determine the structure of the fluid.[55−64] Most of these different approaches use a simple Padé approximant[65,66] for the *u*-expansion for multipolar interactions. Differences between these modifications include the second- and third-order terms in the Padé approximant and the number of additional pure-component parameters for the polar term. For example, Gross[62] developed a new term for dipolar and quadrupolar interactions, where the model constants were adjusted to molecular simulation data without the need of an additional polar interactions parameter. Jog et al.[56,57] developed expressions for dipole−dipole interactions and for quadrupole−

quadrupole interactions based on the work of Larsen et al.[66] They introduced a new adjustable parameter, i.e., the fraction of dipolar segments (or quadrupolar segments) per chain. On the basis of the work of Larsen et al.,[66] Karakatsani et al.[63,64] developed an extended PC-SAFT model for polar interactions, namely the PC-PSAFT. PC-PSAFT is an accurate but rather complex model for real mixture calculations. For this purpose, a truncated version of the model was proposed, known as tPC-PSAFT,[64] which uses an effective polar diameter as an adjustable parameter in order to extend the range of dipolar and quadrupolar interactions beyond the first coordination shell of the polar molecule. Next to dipole−dipole and quadrupole−quadrupole interactions, cross-polar interactions and polarizability effects are also taken into account by both PC-PSAFT and tPC-PSAFT models.

In this work, modeling of the phase behavior of imidazolium-based IL + CO$_2$ systems is based on tPC-PSAFT EoS.[64] It is the first attempt to accurately predict the solubility of CO$_2$ in ILs at high pressures up to 100 MPa.

Model Description

In the PC-SAFT EoS, the reference fluid is the hard-chain fluid, whereas the perturbation accounts for association effects and dispersion interactions. The essence of PC-SAFT is that the residual Helmholtz free energy per mole (a^{res}) is given by a sum of contributions arising from hard-sphere (a^{hs}), chain formation (a^{chain}), association (a^{assoc}), and dispersion (a^{disp}) interactions. In the PC-PSAFT EoS, the model is extended in order to incorporate multipolar interactions. Therefore, an additional perturbation term is added to account for multipolar interactions, a^{polar}, which includes dipole−dipole interactions, quadrupole−quadrupole interactions, and cross dipole−quadrupole interactions:

$$\frac{a^{res}(T, \rho)}{RT} = \frac{a(T, \rho)}{RT} - \frac{a^{ideal}(T, \rho)}{RT}$$

$$= \frac{a^{hs}(T, \rho)}{RT} + \frac{a^{chain}(T, \rho)}{RT} + \frac{a^{disp}(T, \rho)}{RT} + \frac{a^{assoc}(T, \rho)}{RT} + \frac{a^{polar}(T, \rho)}{RT} \quad (1)$$

where T and ρ are the temperature and the molar density of the system, respectively, and R is the universal gas constant. The residual Helmholtz free energy is the difference between the real Helmholtz free energy of the fluid, a, and the Helmholtz free energy for an ideal gas, a^{ideal}, at the same T and ρ. All other thermodynamic properties (pressure, chemical potential, etc.) are calculated from the Helmholtz free energy of the fluid using standard thermodynamic relations.[67]

The hard-sphere term in eq 1 is given by the Carnahan−Starling expression:[68]

$$\frac{a^{hs}}{RT} = m\frac{4\eta - 3\eta^2}{(1 - \eta)^2} \quad (2)$$

In this equation, m is the number of spherical segments per molecule, and η, the reduced density (segment packing fraction), is:

$$\eta = \tau\rho m v^o \quad (3)$$

where $\tau = \pi/6\cdot\sqrt{2} = 0.74078$ and v^o is the temperature-dependent segment molar volume of the fluid, which can be

calculated from the temperature-independent volume of the fluid, v^{oo}, in the following way:[69]

$$v^{\circ} = v^{oo}\left(1 - C \exp\left(-\frac{3u}{kT}\right)\right)^3 \qquad (4)$$

where u/k is the dispersive energy parameter per segment and $C = 0.12$ for all components except hydrogen.[48]

The hard-sphere term contains three pure-component parameters: the number of segments m, the temperature-independent segment volume v^{oo}, and the dispersion energy per segment u/k. Sometimes, the segment diameter σ rather than the segment volume v^{oo} is selected as the pure-component parameter, which can be calculated from the following expression:

$$v^{oo} = \left(\frac{\pi N_A}{6\tau}\right)\sigma^3 \qquad (5)$$

where N_A is Avogadro's number.

For the chain term in eq 1, the following expression is used:[48]

$$\frac{a^{chain}}{RT} = (1 - m)\ln\left(\frac{2 - \eta}{2(1 - \eta)^3}\right) \qquad (6)$$

This equation follows from Wertheim's TPT for association,[47] where association bonds are replaced by covalent, chain-forming bonds. It can be noticed that this term contains the same three pure-component parameters as those used for calculating the hard-sphere contribution. No additional parameter is necessary to account for chain connectivity.

The dispersion contribution to the Helmholtz free energy in eq 1 is given by:[54]

$$\frac{a^{disp}}{RT} =$$
$$-2\pi\rho I_1(\eta, m)m^2\frac{u}{kT}\sigma^3 - \pi\rho m C_1 I_2(\eta, m)m^2\left(\frac{u}{kT}\right)^2\sigma^3 \qquad (7)$$

where C_1 is the following compressibility expression:

$$C_1 = \left(1 + m\frac{8\eta - 2\eta^2}{(1 - \eta)^4} + \right.$$
$$\left.(1 - m)\frac{20\eta - 27\eta^2 + 12\eta^3 - 2\eta^4}{[(1 - \eta)(2 - \eta)]^2}\right)^{-1} \qquad (8)$$

The integrals in the dispersion term are given by the following series expansions:

$$I_1(\eta, m) = \sum_{i=0}^{6} a_i(m)\eta^i \qquad (9)$$

$$I_2(\eta, m) = \sum_{i=0}^{6} b_i(m)\eta^i \qquad (10)$$

where the coefficients a_i and b_i are functions of the chain length m and the universal coefficients a_{ji} and b_{ji} (given by Gross et al.[54]):

$$a_i(m) = a_{0i} + \frac{m - 1}{m}a_{1i} + \frac{m - 1}{m}\frac{m - 2}{m}a_{2i} \qquad (11)$$

$$b_i(m) = b_{0i} + \frac{m - 1}{m}b_{1i} + \frac{m - 1}{m}\frac{m - 2}{m}b_{2i} \qquad (12)$$

Also, for the dispersion term, the same three pure-component parameters are used, and no additional pure-component parameter is required.

The association term in eq 1 is obtained from Wertheim's TPT for association:[47]

$$\frac{a^{assoc}}{RT} = \sum_{A=1}^{M}\left(\ln X^A - \frac{X^A}{2}\right) + \frac{M}{2} \qquad (13)$$

where M is the number of association sites per molecule, and X^A is the mole fraction of molecules not bonded at specific interaction site A. The summation is over all association sites on the molecule. The nonbonded fraction X^A is calculated from:

$$X^A = \frac{1}{1 + \sum_{B=1}^{M} \rho X^B \Delta^{AB}} \qquad (14)$$

where the summation is over all different types of sites, and Δ^{AB} is the association strength, given by:

$$\Delta^{AB} = \sqrt{2}v^{oo}\frac{2 - \eta}{2(1 - \eta)^3}\left[\exp\left(\frac{\epsilon^{AB}}{kT}\right) - 1\right]\kappa^{AB} \qquad (15)$$

In the association term, two new association parameters are introduced: the association energy ϵ^{AB}, and the association volume κ^{AB}. In the mixtures considered in this work, molecules do not self-associate, but they cross-associate. CO_2 is considered to have one association site A^+ (acting as a Lewis acid), while IL is considered to have one association site B^- (acting as a Lewis base). Consequently, eq 14 results to a set of two equations with two unknowns (X^A and X^B) that can be solved analytically.[70] Because no numerical approach was involved, the computational time was considerably reduced compared to the general case of associating mixtures.

The polar term of PC-PSAFT is based on the work of Larsen et al.[66] and has the form of a simple Padé approximant for the Helmholtz free energy:[65,66]

$$\frac{a^{polar}}{RT} = m\frac{a_2^{polar}}{1 - a_3^{polar}/a_2^{polar}} \qquad (16)$$

where the first-order perturbation term vanishes,[71] and a_2^{polar} and a_3^{polar} are the second- and third-order perturbation polar terms, respectively. The third-order term consists of a two-body term ($a_{3,2}^{polar}$) and a three-body term ($a_{3,3}^{polar}$), which both make a significant contribution to the Helmholtz free energy:[72,73]

$$\frac{a_3^{polar}}{RT} = \frac{a_{3,2}^{polar}}{RT} + \frac{a_{3,3}^{polar}}{RT} \qquad (17)$$

Larsen et al.[66] developed accurate expressions for the multipole terms of eq 17 for a hard-sphere fluid. These expressions contain double and triple spatial integrals over the reference fluid that are approximated by third- and fifth-order density polynomials. In PC-PSAFT, Karakatsani et al.[63,64] extended these expressions to chain fluids, both pure components and mixtures. Furthermore, in truncated PC-PSAFT (tPC-PSAFT),[64] the model was simplified considerably by approximating the double and triple integrals with their first-order terms of the corresponding density polynomials. In tPC-PSAFT, an effective polar interaction diameter, σ_p, is introduced. This parameter specifies the transition between the first coordination shell, where the short-range repulsion and hydrogen bonding interactions dominate, and the

CO$_2$ Solubility in Imidazolium-Based Ionic Liquids

J. Phys. Chem. B, Vol. 110, No. 18, 2006 **9265**

region beyond this first coordination shell, where longer-ranged electrostatic polar interactions prevail.[74] The effective polar diameter for various polar compounds (water, methanol, acetone, carbon dioxide) has been reported previously.[75,76] In this work, the effective polar interaction diameter is a model parameter.

As a result, the following expressions are used for the polar interactions:[64]

$$\frac{a_2^{\text{polar}}}{RT} = -\left(\frac{u}{kT}\right)^2 \eta \left[\frac{4}{3}\frac{\tilde{\mu}^4}{(\sigma_p/\sigma)^3} + \frac{12}{5}\frac{\tilde{\mu}^2\tilde{Q}^2}{(\sigma_p/\sigma)^5} + \frac{12}{5}\frac{\tilde{Q}^4}{(\sigma_p/\sigma)^7}\right] \quad (18)$$

$$\frac{a_{3,2}^{\text{polar}}}{RT} = \left(\frac{u}{kT}\right)^3 \eta\tilde{Q}^2 \left[\frac{6}{5}\frac{\tilde{\mu}^4}{(\sigma_p/\sigma)^8} + \frac{144}{175}\frac{\tilde{\mu}^2\tilde{Q}^2}{(\sigma_p/\sigma)^{10}} + \frac{72}{245}\frac{\tilde{Q}^4}{(\sigma_p/\sigma)^{12}}\right] \quad (19)$$

$$\frac{a_{3,3}^{\text{polar}}}{RT} = \left(\frac{u}{kT}\right)^3 \eta^2 \left[\frac{10}{9}\frac{\tilde{\mu}^6}{(\sigma_p/\sigma)^3} + \frac{159}{125}\frac{\tilde{\mu}^4\tilde{Q}^2}{(\sigma_p/\sigma)^5} + \right.$$
$$\left. \frac{689}{1000}\frac{\tilde{\mu}^2\tilde{Q}^4}{(\sigma_p/\sigma)^7} + \frac{243}{800}\frac{\tilde{Q}^6}{(\sigma_p/\sigma)^9}\right] \quad (20)$$

where:

$$\tilde{\mu} = 85.12\frac{\mu/m}{\sqrt{(u/k)\sigma^3}} \quad (21)$$

$$\tilde{Q} = 85.12\frac{Q/m}{\sqrt{(u/k)\sigma^5}} \quad (22)$$

and μ is the dipole moment of the fluid in D and Q is its quadrupole moment in DÅ.

The tPC-PSAFT EoS is extended straightforwardly to mixtures using standard mixing rules. For the dispersion term, the following mixing rules are used:

$$m = \sum_i x_i m_i \quad (23)$$

$$m^2\frac{u}{kT}\sigma^3 = \sum_i\sum_j x_i x_j m_i m_j \left(\frac{u_{ij}}{kT}\right)\sigma_{ij}^3 \quad (24a)$$

$$m^2\left(\frac{u}{kT}\right)^2\sigma^3 = \sum_i\sum_j x_i x_j m_i m_j \left(\frac{u_{ij}}{kT}\right)^2\sigma_{ij}^3 \quad (24b)$$

with:

$$\sigma_{ij} = \frac{1}{2}(\sigma_i + \sigma_j) \quad (25)$$

$$\frac{u_{ij}}{k} = \left(\frac{u_{ii}}{k}\frac{u_{jj}}{k}\right)^{1/2}(1 - k_{ij}) \quad (26)$$

where x_i is the mole fraction of component i, and k_{ij} is the adjustable binary interactions parameter that accounts for the nonideality of the mixture.

The mixing rules for the two-body polar terms (a_2^{polar} and $a_{3,2}^{\text{polar}}$) are:

$$\tilde{\mu} = \frac{\sum_i\sum_j x_i x_j m_i m_j \tilde{\mu}_{ij}}{(\sum_i x_i m_i)^2} \quad (27)$$

$$\tilde{Q} = \frac{\sum_i\sum_j x_i x_j m_i m_j \tilde{Q}_{ij}}{(\sum_i x_i m_i)^2} \quad (28)$$

with:

$$\tilde{\mu}_{ij} = \sqrt{\tilde{\mu}_i\tilde{\mu}_j} \quad (29)$$

$$\tilde{Q}_{ij} = \sqrt{\tilde{Q}_i\tilde{Q}_j} \quad (30)$$

Finally, for the three-body polar term ($a_{3,3}^{\text{polar}}/kT$), the following mixing rules are proposed:

$$\tilde{\mu} = \frac{\sum_i\sum_j\sum_k x_i x_j x_k m_i m_j m_k \tilde{\mu}_{ijk}}{(\sum_i x_i m_i)^3} \quad (31)$$

$$\tilde{Q} = \frac{\sum_i\sum_j\sum_k x_i x_j x_k m_i m_j m_k \tilde{Q}_{ijk}}{(\sum_i x_i m_i)^3} \quad (32)$$

$$\tilde{\Lambda} = (\tilde{\mu}^2\tilde{Q})^{1/3} = \frac{\sum_i\sum_j\sum_k x_i x_j x_k m_i m_j m_k \tilde{\Lambda}_{ijk}}{(\sum_i x_i m_i)^3} \quad (33)$$

$$\tilde{\Gamma} = (\tilde{\mu}\tilde{Q}^2)^{1/3} = \frac{\sum_i\sum_j\sum_k x_i x_j x_k m_i m_j m_k \tilde{\Gamma}_{ijk}}{(\sum_i x_i m_i)^3} \quad (34)$$

with:

$$\tilde{\mu}_{ijk} = (\tilde{\mu}_i\tilde{\mu}_j\tilde{\mu}_k)^{1/3} \quad (35)$$

$$\tilde{Q}_{ijk} = (\tilde{Q}_i\tilde{Q}_j\tilde{Q}_k)^{1/3} \quad (36)$$

$$\tilde{\Lambda}_{ijk} = (\tilde{\mu}_i\tilde{\mu}_j\tilde{Q}_k)^{1/3} \quad (37)$$

$$\tilde{\Gamma}_{ijk} = (\tilde{\mu}_i\tilde{Q}_j\tilde{Q}_k)^{1/3} \quad (38)$$

Parameter Estimation

The tPC-PSAFT EoS contains six pure-component parameters: three parameters for nonassociating nonpolar compounds (i.e., the segment number m, the temperature-independent segment volume v^{oo}, and the segment dispersive energy parameter u/k), two additional parameters for association (i.e., the association energy ϵ^{AB}, and the association volume κ^{AB}), and one additional parameter for polar interactions (i.e., the effective polar interaction diameter σ_p). For nonpolar compounds, the tPC-PSAFT EoS reduces to the original PC-SAFT EoS.

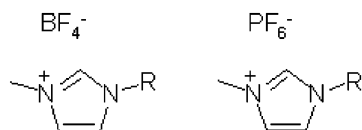**9266** *J. Phys. Chem. B, Vol. 110, No. 18, 2006*

Kroon et al.

Figure 1. Structures of the 1-alkyl-3-methylimidazolium tetrafluoroborate (left) and 1-alkyl-3-methylimidazolium hexafluorophosphate (right) ILs (R = ethyl, butyl, hexyl, octyl,...).

TABLE 1: tPC-PSAFT Parameters for Various Anions and Cations Examined in This Work

	M_w (g/mol)	m (−)	v^oo (ml/mol)	α (Å³)	n (−)	r (Å)	u/k (K)
[BF$_4^-$]	86.80	1.00	28.91	4.41	42	2.25	162.9
[PF$_6^-$]	144.96	1.00	40.95	7.32	70	2.53	223.8
[emim$^+$]	111.17	3.0990	23.31				285.0
[bmim$^+$]	139.22	3.7662	24.72				285.0
[hmim$^+$]	167.28	4.4334	26.14				285.0
[omim$^+$]	195.33	5.1006	27.55				285.0

In this work, the tPC-PSAFT EoS is used to model the phase behavior of IL + CO$_2$ systems. The ILs that are modeled are 1-ethyl-3-methylimidazolium hexafluorophosphate ([emim$^+$]-[PF$_6^-$]), 1-butyl-3-methylimidazolium hexafluorophosphate ([bmim$^+$][PF$_6^-$]), 1-hexyl-3-methylimidazolium hexafluorophosphate ([hmim$^+$][PF$_6^-$]), 1-butyl-3-methylimidazolium tetrafluoroborate ([bmim$^+$][BF$_4^-$]), 1-hexyl-3-methylimidazolium tetrafluoroborate ([hmim$^+$][BF$_4^-$]), and 1-octyl-3-methylimidazolium tetrafluoroborate ([omim$^+$][BF$_4^-$]). In Figure 1, a schematic representation of these ILs is shown. For CO$_2$, the PC-SAFT and tPC-PSAFT pure-component parameters can be found in the literature.[54,62,64] However, the tPC-PSAFT EoS parameters for ILs were unknown and had to be estimated.

Physically meaningful pure-component parameters for ILs (ion pairs) were estimated based on ionic liquid experimental thermodynamic data (density, enthalpy, and entropy of dissolution of CO$_2$) and physicochemical data (size, polarizability, number of electrons) for the constituent ions (cation and anion). The following protocol was used for this purpose. For the anions [BF$_4^-$] and [PF$_6^-$], the size and shape parameters were available in the literature.[77] The dispersive energy parameter for the anions was calculated using the Mavroyannis and Stephen equation:[78]

$$\left(\frac{u}{k}\right)_\text{anion} = 356\frac{\alpha_\text{anion}^{3/2}n_\text{anion}^{1/2}}{r_\text{anion}^6} \tag{39}$$

where α is the polarizability of the anion, n is the number of electrons of the anion, and r is the radius of the anion. The values of α, n, and r for [BF$_4^-$] and [PF$_6^-$] were also found in the literature.[79]

For the size, shape, and energy parameters of the cations [emim$^+$], [bmim$^+$], [hmim$^+$], and [omim$^+$], the PC-SAFT values for ethylbenzene, butylbenzene, hexylbenzene, and octylbenzene, respectively, were used.[54]

In Table 1, the values for the three nonassociating nonpolar parameters for both anions and cations are presented. The size, shape, and energy parameters for the pure total ILs were calculated using standard combining rules:

$$(u/k)_\text{IL} = \sqrt{(u/k)_\text{anion}(u/k)_\text{cation}} \tag{40}$$

$$v_\text{IL}^\text{oo} = \frac{m_\text{anion}v_\text{anion}^\text{oo} + m_\text{cation}v_\text{cation}^\text{oo}}{m_\text{IL}^\text{oo}} \tag{41}$$

where m_IL was fitted to IL density data.[1]

TABLE 2: tPC-PSAFT Pure-Component Parameters for CO$_2$ and Various ILs[a]

	M_w (g/mol)	nonassociating parameters					
		m (−)	v^oo (ml/mol)	u/k (K)	m (D)	Q (DÅ)	σ_p (Å)
CO$_2$	44.01	1.912	9.90	157.97	0.00	4.3	2.974
[emim$^+$][PF$_6^-$]	256.13	3.521	27.61	252.57	1.70	0.00	5.625
[bmim$^+$][PF$_6^-$]	284.18	4.235	28.13	252.57	1.70	0.00	5.660
[hmim$^+$][PF$_6^-$]	312.24	4.834	28.86	252.57	1.70	0.00	5.709
[omim$^+$][PF$_6^-$]	340.29	5.451	29.75	252.57	1.70	0.00	5.767
[emim$^+$][BF$_4^-$]	197.97	3.300	24.67	215.47	1.70	0.00	5.418
[bmim$^+$][BF$_4^-$]	226.02	3.862	25.60	215.47	1.70	0.00	5.485
[hmim$^+$][BF$_4^-$]	254.08	4.417	26.65	215.47	1.70	0.00	5.559
[omim$^+$][BF$_4^-$]	282.13	4.973	27.77	215.47	1.70	0.00	5.636

[a] For the cross-association between CO$_2$ and IL, it is $\epsilon^\text{AB}/k = 2200$ K and $\kappa = 0.0017$ (−)

The polar nature of ILs makes them suitable for solvents in a wide range of chemical processes. Unfortunately, the dipole moment of the ILs examined here is not known experimentally. However, the polarity of various imidazolium-based ILs has been measured by Carmichael et al.[42] using solvatochromic methods and, more recently, by Wakai et al.[80] using dielectric spectroscopy and shown to be comparable to the polarity of lower to medium alcohols. Other experimental measurements for IL mixtures have resulted to similar conclusions that ILs behave as moderately polar organic solvents.[81] Although ionic liquids are larger than lower alcohols, the distance between the positive charge (hydrogen on the C2-position of the cation) and negative charge (fluoride on the anion) within an ionic pair is only 1.914 Å.[82] This distance is slightly larger than the distance between the charges in lower alcohols. On the basis of the above arguments, it is reasonable to assume that ILs have the same dipole moment ($\mu = 1.70$ D) and effective polar interaction diameter ($\sigma_\text{p} = 1.4\ \sigma$) as methanol.[76]

The association parameters for the Lewis acid−base association between the CO$_2$ (Lewis acid) and the anion of the IL (Lewis base) were estimated from literature data[44] for the enthalpy and entropy of dissolution of CO$_2$ in IL using the expressions:[83]

$$\frac{\epsilon^\text{AB}}{k} \approx -\Delta H^\text{dissol} \tag{42}$$

$$\kappa^\text{AB} \approx \exp\left(\frac{\Delta S^\text{dissol}}{R}\right) \tag{43}$$

The resulting values for the energy of association and the volume of association are $\epsilon^\text{AB}/k = 2200$ K, and $\kappa^\text{AB} = 0.0017$ (−), respectively. For comparison, for 1-alcohols larger than 1-butanol, ϵ^AB/k is 2500−2700 K and $\kappa^\text{AB} = 0.0010−0.0013$ (−).[63]

In Table 2, the tPC-PSAFT pure-component parameters for CO$_2$ and ILs are presented. All parameters proposed have a clear physical value. For the homologous series of ILs with increasing alkyl chain, it is also ensured that the parameters vary smoothly with molecular weight (m, v^oo, σ_p) or are constant (u/k, ϵ^AB, κ^AB). For example, in Figure 2, the total volume of the IL equal to $m \cdot v^\text{oo}$ is plotted against the molecular weight of the ionic liquid. As can be seen from this graph, a linear dependence holds, which means that extension to other alkylmethylimidazolium ILs with different alkyl chain length is straightforward.

Results and Discussion

The phase behavior of several alkylmethylimidazolium ILs + CO$_2$ systems is modeled using the tPC-PSAFT EoS and the parameters estimated in the previous section. Only the temper-
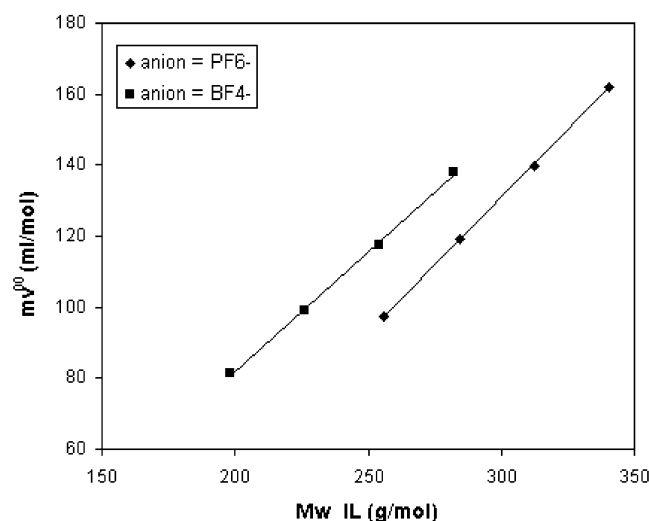
CO₂ Solubility in Imidazolium-Based Ionic Liquids

J. Phys. Chem. B, Vol. 110, No. 18, 2006 **9267**

Figure 2. Total volume of the IL (= $m \cdot v^{oo}$) against the molecular weight of the IL.
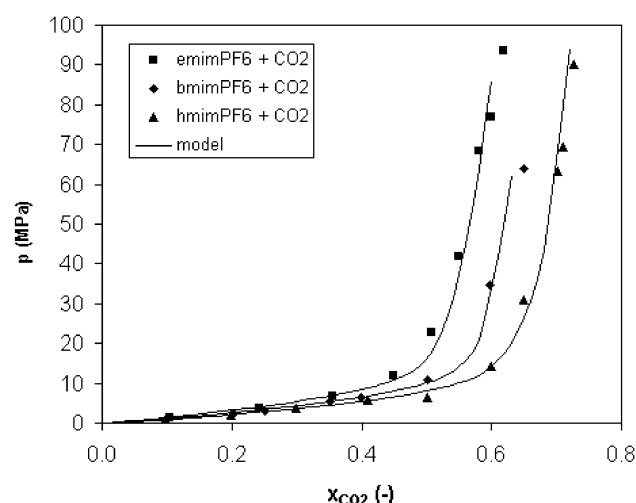

Figure 3. Experimental data[19,20,24] and tPC-PSAFT EoS correlation for the bubble-point pressures of different IL (anion = PF_6^-) + CO₂ systems at 333.15 K.

Figure 4. Dependence of the binary interaction parameter on temperature for different IL (anion = PF_6^-) + CO₂ systems.

Figure 5. Dependence of the binary interaction parameter on molecular weight (alkyl chain length) of IL (anion = PF_6^-) for different temperatures.

TABLE 3: Binary Interaction Parameter for Different IL (Anion = PF_6^-) + CO₂ Mixtures

	binary interaction parameter k_{ij} (−)		
T (K)	[emim⁺][PF₆⁻] + CO₂	[bmim⁺][PF₆⁻] + CO₂	[hmim⁺][PF₆⁻] + CO₂
313.15	0.2027	0.1745	0.1570
323.15	0.2077	0.1794	0.1623
333.15	0.2127	0.1846	0.1675
343.15	0.2184	0.1902	0.1726
353.15	0.2237	0.1954	0.1780

ature-dependent binary interaction parameter k_{ij} is adjusted in order to fit the model to experimental VLE data.

In Figure 3, the bubble-point pressures versus the CO₂ mole fraction for different binary CO₂ + IL (anion = PF_6^-) systems are shown at 333.15 K. Good agreement between experimental data[19,20,24] and the model is observed. It is particularly encouraging that tPC-PSAFT predicts a nearly infinite bubble-point pressure slope at a specific maximum concentration of CO₂ beyond which increasing the external pressure hardly increases the CO₂ solubility in IL, which is in agreement with experiments.[19−23] According to Huang et al.,[29] the reason for this sharp pressure increase at a certain maximum CO₂ concentration is that, at this point, all cavities in the IL phase are occupied by CO₂, so that further insertion of CO₂ would require "breaking" the cohesive structure of the IL. Similarly good agreement between experiment and model was obtained for other temperatures between 313.15 and 353.15 K. A temperature-independent binary interaction parameter was not able to describe the phase behavior accurately over the entire temperature range. A reason for this could be that the association energy is based on a constant enthalpy of dissolution, whereas in reality, the enthalpy of dissolution changes with temperature ($\Delta H \sim RT$). Therefore, when a constant binary interaction parameter is used, the
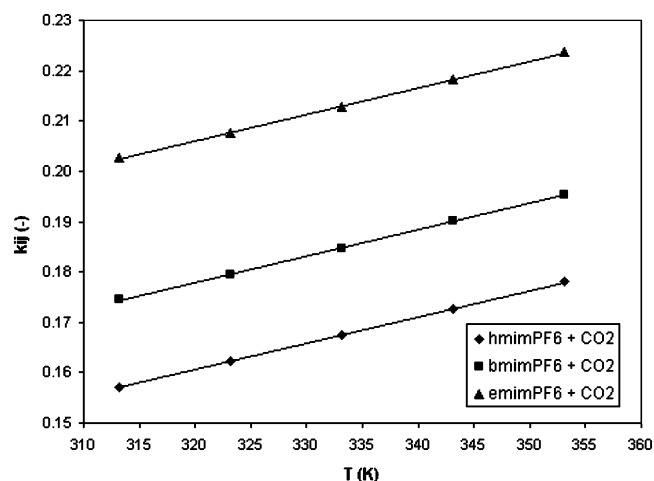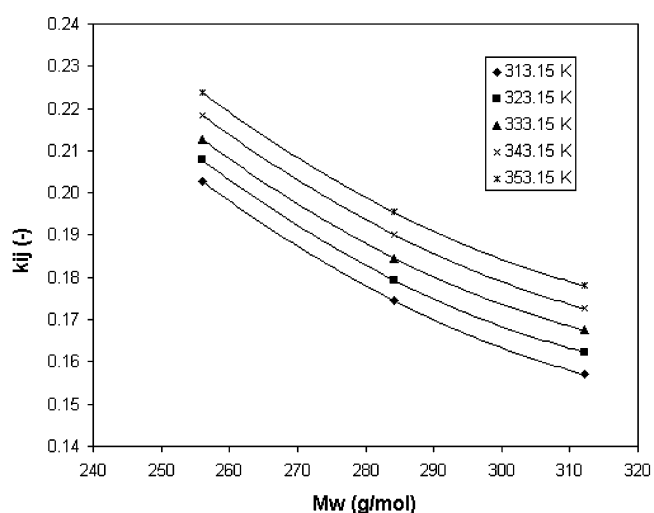
pressure is underpredicted at higher temperatures and overpredicted at lower temperatures. To take the temperature dependence of the enthalpy of dissolution into account, the binary interaction parameter k_{ij} was allowed to vary with temperature. In Table 3, the values for the binary interaction parameter at different temperatures are presented, and in Figures 4 and 5, the dependence of the binary interaction parameter on temperature and molecular weight are shown. The binary interaction parameter increases linearly with temperature and decreases asymptotically with molecular weight. Thus, the lowest k_{ij} values are observed for the ionic liquid + CO₂ mixtures where the alkyl chain is the longest (highest molecular weight) and the temperature is the lowest. This is expected because the deviation from ideal mixing becomes larger at higher temperatures (above
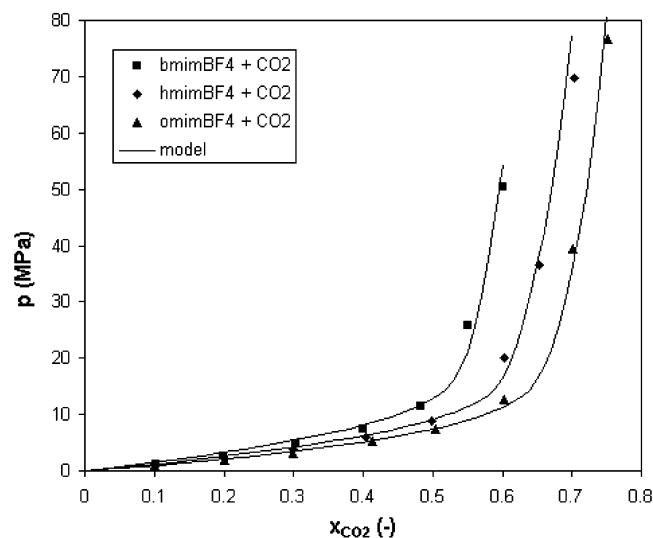
9268 *J. Phys. Chem. B, Vol. 110, No. 18, 2006*

Kroon et al.

Figure 6. Experimental data[21−23] and tPC-PSAFT EoS correlation for the bubble-point pressures of different IL (anion = BF_4^-) + CO_2 systems at 333.15 K.
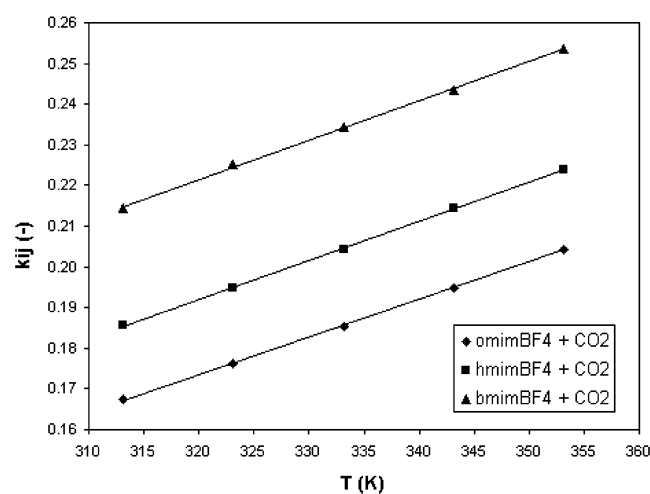

Figure 7. Dependence of the binary interaction parameter on temperature for different IL (anion = BF_4^-) + CO_2 systems
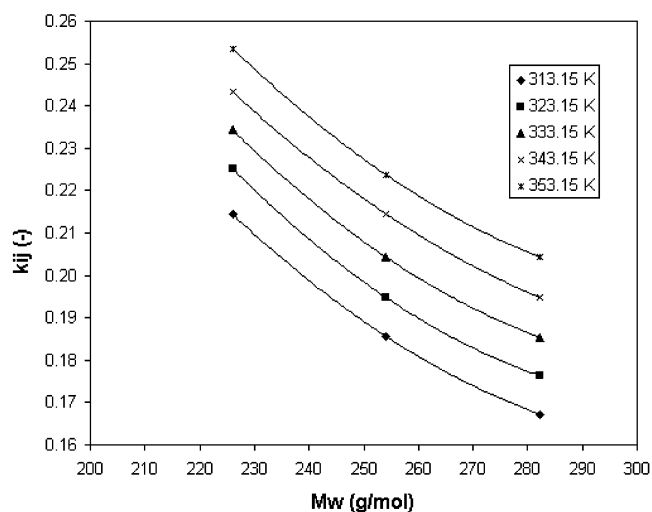

Figure 8. Dependence of the binary interaction parameter on molecular weight (alkyl chain length) of IL (anion = BF_4^-) for different temperatures.
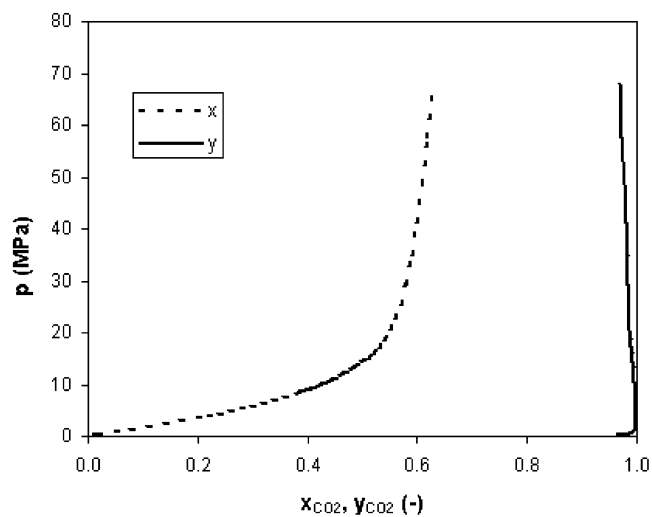

Figure 9. P, x, y − diagram of the $[bmim^+][PF_6^-]$ + CO_2 system at 353.15 K.

TABLE 4: Binary Interaction Parameter for Different IL (Anion = BF_4^-) + CO_2 Mixtures

	binary interaction parameter k_{ij} (−)		
T (K)	$[bmim^+][BF_4^-]$ + CO_2	$[hmim^+][BF_4^-]$ + CO_2	$[omim^+][BF_4^-]$ + CO_2
313.15	0.2144	0.1856	0.1673
323.15	0.2252	0.1948	0.1763
333.15	0.2343	0.2043	0.1854
343.15	0.2433	0.2145	0.1948
353.15	0.2536	0.2237	0.2043

the critical point of CO_2) when the density difference between CO_2 and IL increases. Moreover, in small ionic liquids, the nonideal behavior of the imidazolium ring and anion are dominating, whereas in large ionic liquids, the long alkyl chains (similar to ideal-behaving alkanes) predominate.

The same approach was used to correlate the bubble-point pressures for CO_2 + IL system where the anion is BF_4^-. Again, the binary interaction parameter was allowed to vary with temperature. The results at 333.15 K are shown in Figure 6. Similar plots were obtained for other temperatures between 313.15 and 353.15 K. As can be seen from this figure, the agreement with experimental data[21−23] is good. A similar trend as before is observed for the binary interaction parameter as a function of temperature and of molecular weight (see Figures 7 and 8). However, the temperature dependence of the binary interaction parameter for the $[BF_4^-]$−ionic liquids is larger than the temperature dependence for the $[PF_6^-]$−ionic liquids (see Table 4).

In bubble-point calculations with an EoS, the composition of the vapor phase is calculated also. These have never been measured because it was assumed that ionic liquids have negligible vapor pressure. In Figure 9, the entire P, x, y diagram for the $[bmim^+][[PF_6^-]$ + CO_2 mixture at 353.15 K is shown.

It can be seen that the solubility of carbon dioxide in IL (liquid phase) is high, whereas the solubility of IL in the vapor phase is very low (especially for pressures under 10 MPa), which is in agreement with experimental observations of negligible solubility of ionic liquids in CO_2.[5−7] However, at pressures higher than 10 MPa, the model predicts that some ionic liquid will be present in the supercritical CO_2 phase. Similar predictions were obtained for the other temperatures and the other mixtures examined.

Conclusions

The tPC-PSAFT EoS is able to model the phase behavior of several imidazolium-based IL + CO_2 systems, where the dipolar

CO$_2$ Solubility in Imidazolium-Based Ionic Liquids

J. Phys. Chem. B, Vol. 110, No. 18, 2006 **9269**

interactions between the IL molecules, the quadrupolar interactions between the CO$_2$ molecules, and the Lewis acid−base type of association between the IL molecules and the CO$_2$ molecules are explicitly taken into account. Physically meaningful pure-component parameters were estimated on the basis of literature data and by using standard combining rules. The sole parameter that was fitted to experimental vapor−liquid equilibrium data was the binary interaction parameter. This binary interaction parameter increases linearly with temperature. The best agreement with experimental data and the lowest binary interaction parameter values were observed for IL + CO$_2$ mixtures where the alkyl chain was the longest and the temperature was the lowest.

References and Notes

(1) Wasserscheid, P., Welton, T., Eds. *Ionic Liquids in Synthesis*; Wiley-VCH Verlag: Weinheim, Germany, 2003.

(2) Earle, M. J.; Seddon, K. R. *Pure Appl. Chem.* **2000**, *72*, 1391.

(3) Brennecke, J. F.; Maginn, E. J. *AIChE J.* **2001**, *47*, 2384.

(4) Olivier-Bourbigou, H.; Magna, L. *J. Mol. Catal. A* **2002**, *182−183*, 419.

(5) Blanchard, L. A.; Hancu, D.; Beckman, E. J.; Brennecke, J. F. *Nature* **1999**, *399*, 28.

(6) Blanchard, L. A.; Brennecke, J. F. *Ind. Eng. Chem. Res.* **2001**, *40*, 287.

(7) Blanchard, L. A.; Gu, Z.; Brennecke, J. F. *J. Phys. Chem. B* **2001**, *105*, 2437.

(8) Webb, P. B.; Sellin, M. F.; Kunene, T. E.; Williamson, S.; Slawin, A. M. Z.; Cole-Hamilton, D. J. *J. Am. Chem. Soc.* **2003**, *125*, 15577.

(9) Cole-Hamilton, D. J. *Science* **2003**, *299*, 1702.

(10) Lozano, P.; De Diego, T.; Carrié, D.; Vaultier, M.; Iborra, J. L. *J. Mol. Catal. A* **2004**, *214*, 113.

(11) Dzyuba, S. V.; Bartsch, R. A. *Angew. Chem., Int. Ed.* **2003**, *42*, 148.

(12) Reetz, M. T.; Wiesenhöfer, W.; Franciò, G.; Leitner, W. *Adv. Synth. Catal.* **2003**, *345*, 1221.

(13) Brown, R. A.; Pollet, P.; McKoon, E.; Eckert, C. A.; Liotta, C. L.; Jessop, P. G. *J. Am. Chem. Soc.* **2001**, *123*, 1254.

(14) Anthony, J. L.; Anderson, J. L.; Maginn, E. J.; Brennecke, J. F. *J. Phys. Chem. B* **2005**, *109*, 6366.

(15) Husson-Borg, P.; Majer, V.; Costa Gomes, M. F. *J. Chem. Eng. Data* **2003**, *48*, 480.

(16) Kamps, A. P. S.; Tuma, D.; Xia, J.; Maurer, G. *J. Chem. Eng. Data* **2003**, *48*, 746.

(17) Liu, F.; Abrams, M. B.; Baker, R. T.; Tumas, W. *Chem. Commun.* **2001**, 433.

(18) Camper, D.; Scovazzo, P.; Koval, C.; Noble, R. *Ind. Eng. Chem. Res.* **2004**, *43*, 3049.

(19) Shariati, A.; Peters, C. J. *J. Supercrit. Fluids* **2004**, *29*, 43.

(20) Shariati, A.; Peters, C. J. *J. Supercrit. Fluids* **2004**, *30*, 139.

(21) Constantini, M.; Toussaint, V. A.; Shariati, A.; Peters, C. J.; Kikic, I. *J. Chem. Eng. Data* **2005**, *50*, 52.

(22) Kroon, M. C.; Shariati, A.; Costantini, M.; Van Spronsen, J.; Witkamp, G. J.; Sheldon, R. A.; Peters, C. J. *J. Chem. Eng. Data* **2005**, *50*, 173.

(23) Shariati, A.; Gutkowski, K.; Peters, C. J *AIChE J.* **2005**, *51*, 1532.

(24) Shariati, A.; Peters, C. J. *J. Supercrit. Fluids* **2005**, *34*, 171.

(25) Shah, J. K.; Maginn, E. J. *J. Phys. Chem. B* **2005**, *109*, 10395.

(26) Urukova, I.; Vorholz, J.; Maurer, G. *J. Phys. Chem. B* **2005**, *109*, 12154.

(27) Shah, J. K.; Maginn, E. J. *Fluid Phase Equilib.* **2004**, *222−223*, 195.

(28) Shim, Y.; Choi, M. Y.; Kim, H. J. *J. Chem. Phys.* **2005**, *122*, 044511.

(29) Huang, X.; Margulis, C. J.; Li, Y.; Berne, B. J. *J. Am. Chem. Soc.* **2005**, *127*, 17842.

(30) Lee, S. B. *J. Chem. Technol. Biotechnol.* **2005**, *80*, 133.

(31) Carda-Broch, S.; Berthod, A.; Armstrong, D. W. *Anal. Bioanal. Chem.* **2003**, *375*, 191.

(32) Ally, M. R.; Braunstein, J.; Baltus, R. E.; Dai, S.; DePaoli, D. W.; Simonson, J. M. *Ind. Eng. Chem.* Res. **2004**, *43*, 1296.

(33) Scovazzo, P.; Camper, D.; Kieft, J.; Poshusta, J.; Koval, C.; Noble, R. *Ind. Eng. Chem. Res.* **2004**, *43*, 6855.

(34) Shiflett, M. B.; Yokozeki, A. *Ind. Eng. Chem. Res.* **2005**, *44*, 4453.

(35) Shariati, A.; Peters, C. J. *J. Supercrit. Fluids* **2003**, *25*, 109.

(36) Belvèze, L. S.; Brennecke, J. F.; Stadtherr, M. A. *Ind. Eng. Chem. Res.* **2004**, *43*, 815.

(37) Rebelo, L. P. N.; Najdanovic-Visak, V.; Visak, Z. P.; Nunes da Ponte, M.; Szydlowski, J.; Cerdeiriña, C. A.; Troncoso, J.; Romaní, L.; Esperança, J. M. S. S.; Guedes, H. J. R.; De Sousa, H. C. *Green. Chem.* **2004**, *6*, 369.

(38) Banerjee, T.; Singh, M. K.; Kumar Sahoo, R.; Khanna, A. *Fluid Phase Equilib.* **2005**, *234*, 64.

(39) Katsyuba, S. A.; Dyson, P. J.; Vandyukova, E. E.; Chernova, A. V.; Vidiš, A. *Helv. Chim. Acta* **2004**, *87*, 2556.

(40) Anthony, J. H.; Mertens, D.; Breitenschein, T.; Dölle, A.; Wasserscheid, P.; Carper, W. R. *Pure Appl. Chem.* **2004**, *76*, 255.

(41) Paulechka, Y. U.; Kabo, G. J.; Blokhin, A. V.; Vydrov, O. A.; Magee, J. M.; Frenkel, M. *J. Chem. Eng. Data* **2003**, *48*, 457.

(42) Carmichael, A. J.; Seddon, K. R. *J. Phys. Org. Chem.* **2000**, *13*, 591.

(43) Buckingham, A. D.; Disch, R. L. *Proc. R. Soc. London, Ser. A* **1963**, *273*, 275.

(44) Cadena, C.; Anthony, J. L.; Shah, J. K.; Morrow, T. I.; Brennecke, J. F.; Maginn, E. J. *J. Am. Chem.* Soc. **2004**, *126*, 5300.

(45) Kazarian, S. G.; Briscoe, B. J.; Welton, T. *Chem. Commun.* **2000**, *20*, 2047.

(46) Chapman, W. G.; Gubbins, K. E.; Jackson, G.; Radosz, M. *Fluid Phase Equilib.* **1989**, *52*, 31.

(47) Chapman, W. G.; Gubbins, K. E.; Jackson, G.; Radosz, M. *Ind. Eng. Chem. Res.* **1990**, *29*, 1709.

(48) Huang, S. H.; Radosz, M. *Ind. Eng. Chem. Res.* **1990**, *29*, 2284.

(49) Huang, S. H.; Radosz, M. *Ind. Eng. Chem. Res.* **1991**, *30*, 1994.

(50) Wertheim, M. S. *J. Stat. Phys.* **1984**, *35*, 19.

(51) Wertheim, M. S. *J. Stat. Phys.* **1984**, *35*, 35.

(52) Wertheim, M. S. *J. Stat. Phys.* **1986**, *42*, 459.

(53) Wertheim, M. S. *J. Stat. Phys.* **1986**, *42*, 477.

(54) Gross, J.; Sadowski, G. *Ind. Eng. Chem. Res.* **2001**, *40*, 1244.

(55) Walsh, J. M.; Guedes, H. J. R.; Gubbins K. E. *J. Phys. Chem.* **1992**, *96*, 10995.

(56) Jog, P. K.; Chapman, W. G. *Mol. Phys.* **1999**, *97*, 307.

(57) Jog, P.; Sauer, S.; Blaesig, J.; Chapman, W. G. *Ind. Eng. Chem. Res.* **2001**, *40*, 4641.

(58) Sauer, S. G.; Chapman, W. G. *Ind. Eng. Chem. Res.* **2003**, *42*, 5687.

(59) Chapman, W. G.; Sauer, S. G.; Ting, D.; Ghosh, A. *Fluid Phase Equilib.* **2004**, *217*, 137.

(60) Tumakaka, F.; Sadowski, G. *Fluid Phase Equilib.* **2004**, *217*, 233.

(61) Tumakaka, F.; Gross, J.; Sadowski, G. *Fluid Phase Equilib.* **2005**, *228−229*, 89.

(62) Gross, J. *AIChE J.* **2005**, *51*, 2556.

(63) Karakatsani, E. K.; Spyriouni, T.; Economou, I. G. *AIChE J.* **2005**, *51*, 2328.

(64) Karakatsani, E. K.; Economou, I. G. *J. Phys. Chem. B* **2006**, *110*, 9252.

(65) Stell G.; Rasaiah, J. C.; Narang, H. *Mol Phys.* **1974**, *27*, 1393.

(66) Larsen, B.; Rasaiah, J. C.; Stell, G. *Mol. Phys.* **1977**, *33*, 987.

(67) Prausnitz, J. M.; Lichtenthaler, R. N.; Gomes de Azevedo, E. *Molecular Thermodynamics of Fluid-Phase Equilibria*, 3rd ed.; Prentice Hall: Englewood Cliffs, NJ, 1999.

(68) Carnahan, N. F.; Starling, K. E. *J. Chem. Phys.* **1969**, *51*, 635.

(69) Chen, S. S.; Kreglewski, A. *Ber. Bunsen-Ges. Phys. Chem.* **1977**, *81*, 1048.

(70) Kraska, T. *Ind. Eng. Chem. Res.* **1998**, *37*, 4889.

(71) Vega, C. *Mol. Phys.* **1992**, *75*, 427.

(72) Rasaiah, J. C.; Stell. G. *Chem. Phys. Lett.* **1974**, *25*, 519.

(73) Stell, G.; Rasaiah, J. C.; Narang, H. *Mol. Phys.* **1974**, *27*, 1393.

(74) Nezbeda, I. *Czech. J. Phys.* **1998**, *48*, 117.

(75) Kolafa, J.; Nezbeda, I. *Mol. Phys.* **2000**, *98*, 1505.

(76) Kettler, M.; Nezbeda, I.; Chialvo, A. A.; Cummings, P. T. *J. Phys. Chem. B* **2002**, *106*, 7537.

(77) McEwen, A. B.; Ngo, H. L.; LeCompte, K.; Goldman, J. L. *J. Electrochem. Soc.* **1999**, *146*, 1687.

(78) Mavroyannis, C.; Stephen, M. J. *Mol. Phys.* **1962**, *5*, 629.

(79) Lide, D. R.; Ed. *Handbook of Chemistry and Physics*, 78th ed.; CRC Press: New York, 1997.

(80) Wakai, C.; Oleinikova, A.; Ott, M.; Weingärtner, H. *J. Phys. Chem. B* **2005**, *109*, 17028.

(81) Znamenskiy, V.; Kobrak, M. N. *J. Phys. Chem. B* **2004**, *108*, 1072.

(82) Meng, Z.; Dölle, A.; Carper, W. R. *J. Mol. Struct. (THEOCHEM)* **2002**, *585*, 119.

(83) Wolbach, J. P.; Sandler, S. I. *Ind. Eng. Chem. Res.* **1998**, *37*, 2917.